23rd ABCM International Congress of Mechanical Engineering
December 6-11, 2015, Rio de Janeiro, RJ, Brazil

INFLUENCE OF ELASTIC FORCES IN TRANSITION PHENOMENON

Analice Costacurta Brandi
Ellen Silva Gervazoni
Faculdade de Ciências e Tecnologia, Universidade Estadual Paulista "Júlio de Mesquita Filho"
Rua Roberto Simonsen, 305
19060-900, Presidente Prudente - SP
analice@fct.unesp.br, ellengerva@gmail.com

Márcio Teixeira de Mendonça
Instituto de Aeronáutica e Espaço, Divisão de Propulsão Aeronáutica - CTA/IAE/APA
Pç Marechal Eduardo Gomes, 50
12228-904, São José dos Campos, SP
marciomtm@iae.cta.br

Leandro Franco de Souza
Instituto de Ciências Matemáticas e de Computação, Universidade de São Paulo
Av. Trabalhador São Carlense, 400
13566-590, São Carlos - SP
lefraso@icmc.usp.br

Abstract. *Several flows of practical interest are of non-newtonian fluids and it is often desirable to know if these flows are in a laminar or turbulent state. A class of these fluids is classified as viscoelastic fluids. In this paper the growth rate of Tollmien-Schlichting waves is studied for Poiseuille flow for a non-Newtonian fluid. The mathematical model adopted for the non-Newtonian fluid extra-stress tensor is the Oldroyd-B. The analysis is carried out by means of Direct Numerical Simulation. The Navier-Stokes equations along with the Oldroyd-B constitutive equation are solved using a high-order finite differences numerical model. The results show that the amplification rates obtained differs from Newtonian fluid as the Weissenberg number increases. Comparisons are presented considering the maximum amplification rates for Newtonian and non-Newtonian fluid for different values of dimensionless parameters.*

Keywords: *laminar-turbulent transition, viscoelastic fluids, Poiseuille Flow, Direct Numerical Simulation*

1. INTRODUCTION

Computational fluid dynamics is an area of significant industrial interest in the chemical, food and oil fields. Among the various problems that have arisen in this area is the treatment of non-Newtonian fluids flows, since viscoelastic fluids find application in many industrial processes and theirs study represents a great challenge. Therefore, a great deal of effort has been expended over the last twenty years or so in attempting to find robust and stable numerical methods for viscoelastic flow problems. However, this is not an easy work because the viscoelastic fluid constitutive equations are complex mathematical equations and are difficult to treat in computationally.

There are many scientific and industrial applications where the laminar flow stability and transition to turbulence are relevant. It is important to investigate the physics of stability and laminar-turbulent transition to control, advance or prevent it. A great effort has been expended in recent years to gain more knowledge in this area. There has been much work on channel flows of viscoelastic fluids in the literature. Poiseuille flow and Couette flow are often used as benchmark tests for new constitutive equations (Han (1976)) and there has been much interest in instabilities in Couette flow of viscoelastic fluids since Gorodtsov and Leonov (1967) calculated two modes. Poiseuille flows however, do not appear to have been so comprehensively covered, although has some studies of the literature.

The planar Poiseuille flow of a Newtonian fluid is an elementary mathematical problem. Instabilities in multilayered Poiseuille flows are another matter however. In 1967 Yih showed that viscosity stratification across two Newtonian fluids in Poiseuille flow can cause instability (Yih (1967)). The unstable modes were discovered to be in the region of a previously known neutral mode for the single fluid case, hence implying the importance of an investigation of the full eigenspectrum as opposed to considering only unstable modes. A stability analysis of planar Poiseuille flow of a non-Newtonian fluid was performed by Porteous and Denn in 1972 (Porteous and Denn (1972a), Porteous and Denn (1972b)). The viscoelastic fluid models of a second-order fluid and a Maxwell fluid were investigated and a new elastic mode of the Orr-Sommerfeld equation was determined. Elasticity was found to be destabilizing for finite disturbances.

An investigation of numerical instabilities occurring in time-dependent simulation of planar Couette flow for the upper-convected Maxwell, Oldroyd-B and FENE equations were investigated by Keiller in 1992 (Keiller (1992)). For creeping flow it is shown that the poor resolution of a continuous spectrum of singular eigenfunctions may lead to an instability criterion We_{crit}. Thus the limiting Weissenberg number is determined not by the absolute refinement of the grid but the relative refinement in the cross-stream to streamwise directions. Some results presented for time dependent entry flow simulations suggests that We_{crit} may depend on the relative refinement of the grid in this flow also. This instability is less severe for the FENE equation and this is attributed to the lower normal stresses for this equation.

According to Sureshkumar *et al.* (1999), the linear stability analysis in complex viscoelastic fluid flows become extremely complicated by the hyperbolic nature of the constitutive differential equations. Furthermore, the presence of boundary layers of elastic tension require discretization methods capable of capturing abrupt changes in disturbed fields and require extremely fine mesh, becoming of high computational cost.

A study of local linear stability analyses of viscous and viscoelastic flows through a periodically constricted channel has been undertaken by Sureshkumar (Sureshkumar (2001)). Stability analysis of such non-viscometric flows is a computationally demanding task since both streamwise and wall-normal directions are spatially inhomogeneous, thereby ruling out closed form solutions for the base flow. Linear stability analysis was performed locally, i.e. by treating the axial position as a parameter. For a given set of geometric and disturbance parameters, the most dangerous axial position was identified as the location for which the most dangerous eigenvalue has the largest real part. The upper convected Maxwell (UCM) model was chosen as a viscoelastic constitutive equation, since the primary objective was to qualitatively assess the influence of elasticity on the linear stability of the shear layer. For comparison purposes, linear stability analysis was also performed for the second order fluid (SOF) model for a limited range of parameters.

Palmer in 2007 has studied a one-dimensional planar channel through which the viscoelastic fluid experiences pressure driven Poiseuille flow. Two viscoelastic fluid models, the Giesekus and linear Phan-Thien Tanner (PTT) models, were investigated in one-, two- and three-layered flows and the eigenspectra were sought, with the intention of investigating any instabilities which arise (Palmer (2007)).

Recently Zhang *et al.* has investigated the modal and non-modal stability of both FENE-P and Oldroyd-B fluids in channel flow. FENE-P includes an upper bound for the extension of polymer molecules and can more reliably represent dilute polymer solutions where significant drag reduction in the turbulent regime is observed. A complete study was presented in order to illustrate the effects of the different rheological parameters on the flow stability. The results were verified and examined by means of an energy budget analysis. The stability analysis of the FENE-P Poiseuille flow in the inertia-dominated regime, $Re > 2000$ was investigated (Zhang *et al.* (2013)). The only linear stability analyses of the FENE-P fluids have been performed by Arora and Khomami (Arora and Khomami (2005)) and very recently by Lieu *et al.* (Lieu *et al.* (2013)) on the inertialess regime of Couette flow.

In this work, we are concerned with numerical simulation of two-dimensional viscoelastic fluid flow using the Oldroyd-B constitutive equation. We deal specifically with the investigation of the Tollmien-Schlichting waves convection in a plane Poiseuille flow. The governing equations are written in a vorticity-velocity formulation. The analysis is carried out by means of Direct Numerical Simulation (DNS). The linear system arising from the numerical solution of the Poisson equation is solved by a multigrid methods. The spatial derivatives are discretized by compact finite difference schemes. The time integration is carried out by a fourth-order Runge-Kutta method. In order to evaluate the maximum amplification rates, different values of dimensionless parameters are tested for Newtonian and non-Newtonian fluid flows.

2. MATHEMATICAL FORMULATION

The flow is assumed to be unsteady, non-newtonian, two-dimensional and incompressible. The governing equations are the continuity and Navier-Stokes equations with a constitutive relation for the non-Newtonian extra-stress tensor, that in this work is considered the Oldroyd-B constitutive equation. The basic conservation equations governing the flow are:

$$\nabla \cdot \mathbf{u} = 0, \tag{1}$$

$$\rho \left(\frac{\partial \mathbf{u}}{\partial t} + \nabla \cdot (\mathbf{u}\mathbf{u}) \right) = -\nabla p + \nabla \cdot \mathbf{T} + \rho\, \mathbf{g}, \tag{2}$$

where $\mathbf{u}$ denotes the velocity field, t is the time, ρ is the fluid density, p is the pressure, $\mathbf{T}$ is the extra-stress tensor and $\mathbf{g}$ is the gravitational field. In this paper we worked with viscoelastic flows governed by the non-linear constitutive equation Oldroyd-B (Crochet *et al.* (1984)), that is given by

$$\mathbf{T} + \lambda \overset{\nabla}{\mathbf{T}} = 2\eta \mathbf{D}, \tag{3}$$

where $\mathbf{D} = \frac{1}{2}(\nabla \mathbf{u} + (\nabla \mathbf{u})^T)$ is the rate of deformation tensor, λ is the relaxation-time of the fluid, η is the polymer-contributed viscosity and $\overset{\nabla}{\mathbf{T}}$ is the upper-convected derivative of $\mathbf{T}$ defined by

$$\overset{\nabla}{\mathbf{T}} = \frac{\partial \mathbf{T}}{\partial t} + \nabla \cdot (\mathbf{u}\mathbf{T}) - \mathbf{T} \cdot (\nabla \mathbf{u})^T - (\nabla \mathbf{u}) \cdot \mathbf{T}.$$

Equations (1)–(3) have been non-dimensionalized with the following scalings:

$$\mathbf{x}^* = \frac{x}{L}, \quad \mathbf{u}^* = \frac{\mathbf{u}}{U}, \quad t^* = \frac{U}{L}t, \quad p^* = \frac{p}{\rho U^2}, \quad \mathbf{T}^* = \frac{\mathbf{T}}{\rho U^2}, \tag{4}$$

where L and U denote length and velocity scales, respectively. These equations can then be written (omitting the symbol $*$ for convenience) as

$$\nabla \cdot \mathbf{u} = 0, \tag{5}$$

$$\frac{\partial \mathbf{u}}{\partial t} + \nabla \cdot (\mathbf{uu}) = -\nabla p + \frac{\beta}{Re}\nabla^2 \mathbf{u} + \nabla \cdot \mathbf{T}, \tag{6}$$

$$\mathbf{T} + We\overset{\nabla}{\mathbf{T}} = 2\frac{(1-\beta)}{Re}\mathbf{D}, \tag{7}$$

where the dimensionless parameters $Re = \dfrac{\rho U L}{\eta}$ and $We = \dfrac{\lambda U}{L}$ denote the associated Reynolds and Weissenberg numbers, respectively. The amount of Newtonian solvent is controlled by the dimensionless solvent viscosity coefficient, $\beta = \dfrac{\eta_s}{\eta_0}$, where $\eta_0 = \eta_s + \eta_p$ denotes the total shear viscosity; η_s and η_p represent the newtonian solvent and polymeric viscosities, respectively.

In order to eliminate the treatment of the pressure in the Navier-Stokes equations, we opted for the use of vorticity-velocity formulation. Therefore, Eqs. (5)–(7) can be written as

$$\frac{\partial u}{\partial x} + \frac{\partial v}{\partial y} = 0, \tag{8}$$

$$\frac{\partial^2 v}{\partial x^2} + \frac{\partial^2 v}{\partial y^2} = -\frac{\partial \omega_z}{\partial x}, \tag{9}$$

$$\frac{\partial \omega_z}{\partial t} + \frac{\partial (u\omega_z)}{\partial x} + \frac{\partial (v\omega_z)}{\partial y} = \frac{\beta}{Re}\left(\frac{\partial^2 \omega_z}{\partial x^2} + \frac{\partial^2 \omega_z}{\partial y^2}\right) + \frac{\partial^2 T^{xx}}{\partial x \partial y} + \frac{\partial^2 T^{xy}}{\partial y^2} - \frac{\partial^2 T^{xy}}{\partial x^2} - \frac{\partial^2 T^{yy}}{\partial x \partial y}, \tag{10}$$

$$T^{xx} + We\left(\frac{\partial T^{xx}}{\partial t} + \frac{\partial (uT^{xx})}{\partial x} + \frac{\partial (vT^{xx})}{\partial y} - 2T^{xx}\frac{\partial u}{\partial x} - 2T^{xy}\frac{\partial u}{\partial y}\right) = 2\frac{(1-\beta)}{Re}\frac{\partial u}{\partial x}, \tag{11}$$

$$T^{xy} + We\left(\frac{\partial T^{xy}}{\partial t} + \frac{\partial (uT^{xy})}{\partial x} + \frac{\partial (vT^{xy})}{\partial y} - T^{xx}\frac{\partial v}{\partial x} - T^{yy}\frac{\partial u}{\partial y}\right) = \frac{(1-\beta)}{Re}\left(\frac{\partial v}{\partial x} + \frac{\partial u}{\partial y}\right), \tag{12}$$

$$T^{yy} + We\left(\frac{\partial T^{yy}}{\partial t} + \frac{\partial (uT^{yy})}{\partial x} + \frac{\partial (vT^{yy})}{\partial y} - 2T^{xy}\frac{\partial v}{\partial x} - 2T^{yy}\frac{\partial v}{\partial y}\right) = 2\frac{(1-\beta)}{Re}\frac{\partial v}{\partial y}, \tag{13}$$

where u and v represent the velocity components in longitudinal and normal directions, respectively and ω_z represents the vorticity. Taking this formulation into consideration, the system to be solved consists of the Eqs. (8)–(13). The boundary conditions are specified according to the problem under consideration.

3. NUMERICAL METHOD

The system of equations (8)–(13) is solved numerically in the domain as shown in Fig. 1. The calculations are done on an orthogonal uniform grid, parallel to the wall. The fluid enters the computational domain at $x = x_0$ and exits at the outflow boundary $x = x_{max}$. In this work, the behavior of infinitesimal disturbances in the flow is investigated. Steady disturbances are introduced into the flow field using suction and blowing of mass at the walls (Fasel *et al.* (1990)). This strip is located between x_1 and x_2.

At the beginning, in the time $t = 0$ the flow is undisturbed, therefore from a time $t > 0$, the disturbances are introduced in a region near the inflow, known as disturbance strip, through the imposition of the v velocity:

$$v = Af(x)\, sin(\omega_t\, t), \quad x_1 < x < x_2, \tag{14}$$

and

$$v = 0, \quad x \leq x_1 \quad \text{or} \quad x \geq x_2, \tag{15}$$

where A is a constant used to adjust the amplitude of the disturbances, $f(x)$ is a 9th-order function, ω_t is the disturbance temporal frequency and the points x_1 and x_2 are the initial and the last point of the disturbance strip. The values of $f(x)$, its first, and second derivatives are zero in these extreme points. In the region located between x_0 and x_1 and x_3 and x_4

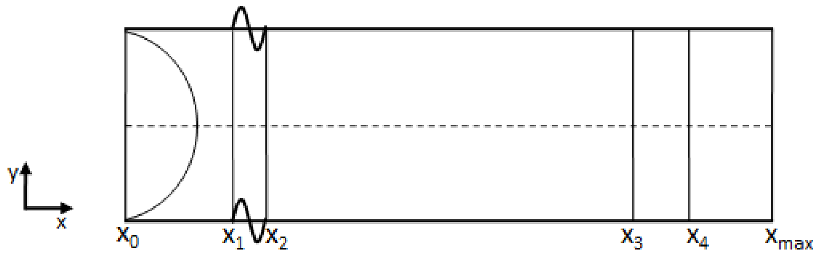

Figure 1. Definition of the computational domain for 2D Poiseuille flow.

a buffer domain technique, from Kloker *et al.* (1993), is implemented in order to avoid wave reflections from the inflow and outflow boundaries, respectively.

The time derivatives in the vorticity transport and the components of the non-Newtonian extra-stress tensor equations are discretized with a classical four step fourth-order Runge-Kutta integration scheme (Ferziger and Peric (1997)). The spatial derivatives are calculated using a high-order compact finite difference-schemes (Souza *et al.* (2005); Souza (2003); Lele (1992); Kloker (1998)). The use of the adopted compact finite differences to estimate the first and second spatial derivatives requires the solution of tridiagonal linear systems. The numerical derivative approximations have 5th- and 6th-order of accuracy (Souza *et al.* (2005)). The Poisson equation is solved using a multigrid Full Approximation Scheme (FAS) (Stüben and Trottenberg (1981)).

Finally, with the purpose of eliminating numerical (spurious) oscillations, a filter is applied after the last Runge-Kutta step. The filter adopted requires the solution of a pentadiagonal system. This filter is applied in the vorticity component in the streamwise direction and in the non-Newtonian extra-stress tensor components.

We solve Eqs. (8)–(13) numerically by the application of the following algorithm:
Step 1: Apply a step of the time integrator.
Step 2: Apply the functions responsible for the damping and relaminarization zones.
Step 3: Introduce the disturbances by suction and blowing at the walls.
Step 4: Calculate the right hand side of Eq. (9).
Step 5: Calculate the v velocity by solving the Poisson equation [Eq. (9)].
Step 6: Calculate the value of u velocity through Eq. (8).
Step 7: Calculate the ω_z vorticity through Eq. (10).
Step 8: Calculate the components of the non-Newtonian extra-stress tensor through Eqs. (11)–(13).
Step 9: Update the vorticity value ω_z and the components of the non-Newtonian extra-stress tensor at the walls.
Step 10: Apply the filter after the last sub-step of the time integrator.

The numerical simulation finishes when the desired wall clock time is reached.

4. NUMERICAL RESULTS

The parameters adopted in the simulations carried out here were: Reynolds number $Re = 10000$; disturbance frequency $\omega_t = 0.27$, 729 points in the streamwise direction, 129 points in the wall normal direction; distance between two consecutive points in the streamwise and wall normal directions: $dx = 0.1793$ and $dy = 0.015625$, respectively. The time step adopted was $dt = 0.2424$. The parameter A to adjust the amplitude of the Tollmien-Schlichting waves was 1×10^{-4}. The disturbances were introduced between points 40 and 72, and the buffer domain initiates in point 629 until point 689. This case was chosen because it is nearly a neutral case for Newtonian fluid, therefore allow a good comparison when non-Newtonian terms are added to the equations. This case was also adopted in the work of Rogenski *et al.* in 2014 (Rogenski *et al.* (2015)).

Figure 2 shows the development of the maximum disturbance velocity U_{max} in the streamwise direction (x) obtained by time Fourier analysis. In this figure the Weissenberg was fixed to $We = 1.0$. The solid line shows the behavior of the TS waves of the Newtonian fluid. It can be seem that the disturbances remains with almost the same level in all the domain, as expected for a nearly neutral case. Three other cases with different β values are also shown $\beta = 0.2, 0.5$ and 0.8. These results shows that as the β increase the flow becomes more unstable.

The Weissenberg number (We) effect is shown in Fig. 3 for $\beta = 0.8$. The flow becomes more unstable increasing the Weissenberg number. Although the growth rate is very small for this β, it can be seem that the fluid becomes more unstable to disturbances with higher Weissenberg numbers.

Figure 4 shows the development of TS waves with $\beta = 0.5$. In the present case the fluid is composed by half Newtonian and half non-Newtonian parts. The effect of the Weissenberg number in these results are more pronounced than the previous case ($\beta = 0.8$).

The last results shown here were obtained for $\beta = 0.2$. With this β number only two Weissenberg numbers were

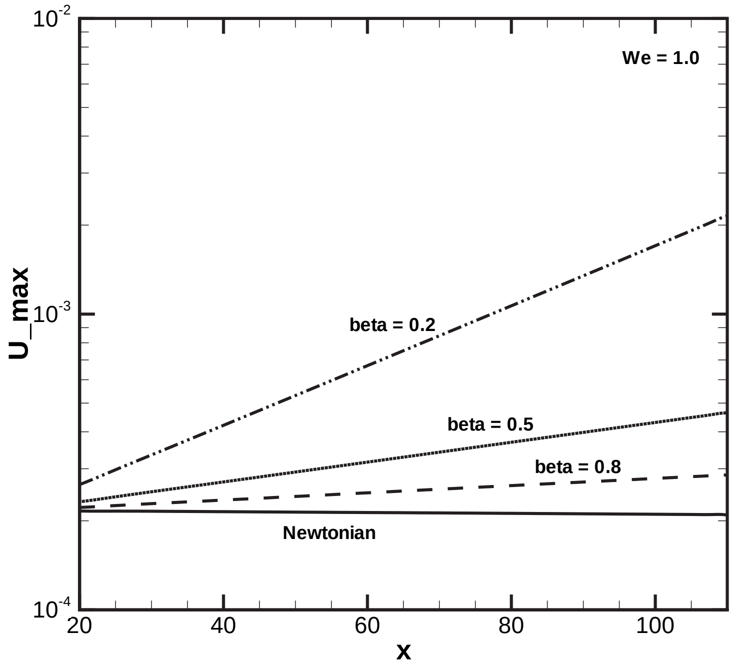

Figure 2. Maximum streamwise velocity disturbance development in the streamwise direction. Weissenberg number = 1.0. Solid line - Newtonian fluid, dashed line - $\beta = 0.8$, dotted line - $\beta = 0.5$, dash point line - $\beta = 0.2$.

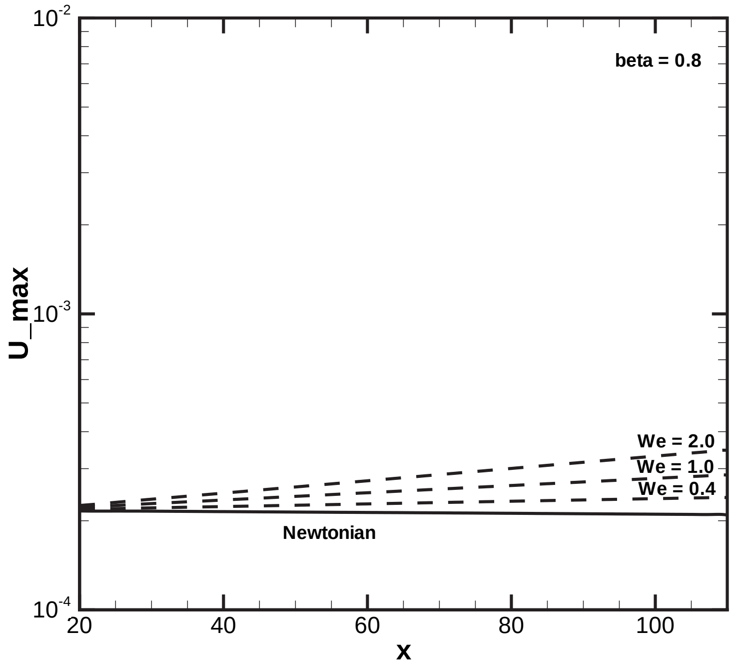

Figure 3. Maximum streamwise velocity disturbance development in the streamwise direction. $\beta = 0.8$. Solid line - Newtonian fluid, dashed lines - $We = 0.4, 1.0$ and 2.0.

simulated. The results are in agreement with the above obtained results, the growth rate (the rate that the disturbances grow i.e. derivative of the curves in the streamwise direction) of disturbances increases with Weissenberg number.

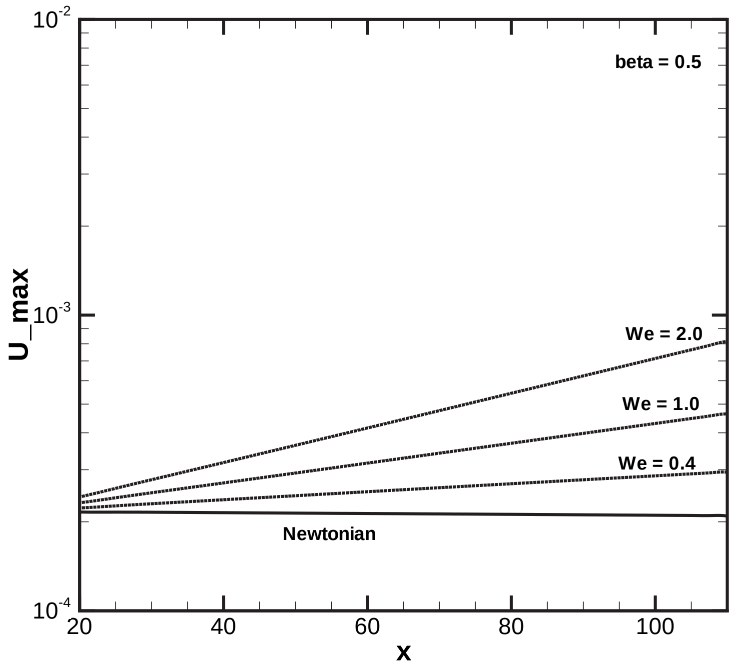

Figure 4. Maximum streamwise velocity disturbance development in the streamwise direction. $\beta = 0.5$. Solid line - Newtonian fluid, dotted lines - $We = 0.4, 1.0$ and 2.0.

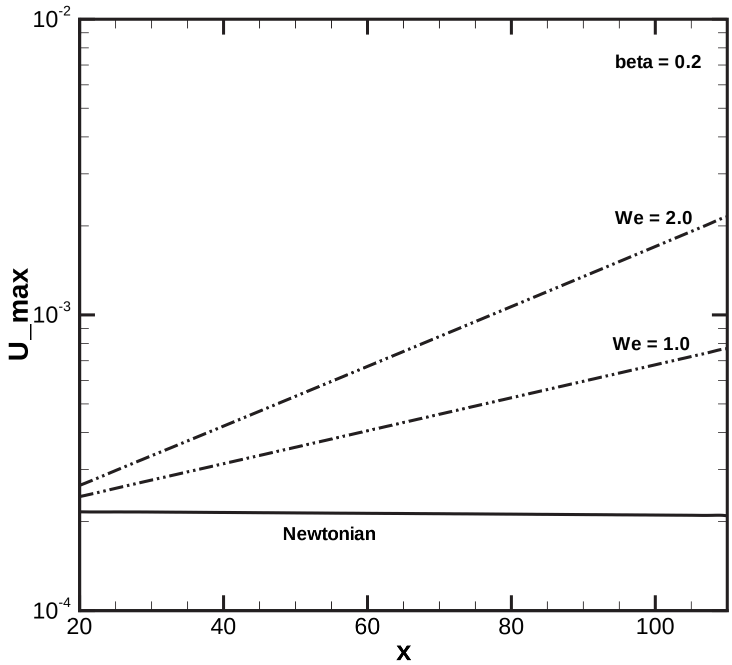

Figure 5. Maximum streamwise velocity disturbance development in the streamwise direction. $\beta = 0.2$. Solid line - Newtonian fluid, dashdotted lines - $We = 1.0$ and 2.0.

5. CONCLUSIONS

In this paper a Direct Numerical Simulation was performed to investigate of the Tollmien-Schlichting waves convection in a plane Poiseuille flow. For this numerical simulation of two-dimensional viscoelastic fluid flow using the

Oldroyd-B constitutive equation was carried out. The governing equations are written in a vorticity-velocity formulation. In order to evaluate the maximum amplification rates, different values of dimensionless parameters are tested for Newtonian and non-Newtonian fluid flows.

The results obtained shows that the flow becomes more unstable to unsteady disturbances as the β number increases, and also shows that the growth rate of the flows increases with the Weissenberg number.

6. REFERENCES

Arora, K. and Khomami, B., 2005. "The influence of finite extensibility on the eigenspectrum of dilute polymeric solutions". *Journal of Non-Newtonian Fluid Mechanics*, Vol. 129, pp. 56–60.

Crochet, M., Davis, A.R. and Walters, K., 1984. *Numerical Simulation of Non-Newtonian Flow*. Elsevier, New York.

Fasel, H.F., Rist, U. and Konzelmann, U., 1990. "Numerical investigation of the three-dimensional development in boundary-layer transition". *AIAA*, Vol. **28**, pp. 29–37.

Ferziger, J.H. and Peric, M., 1997. *Computational Methods for Fluid Dynamics*. Springer-Verlag Berlin Heidelberg New York.

Gorodtsov, V.A. and Leonov, A.I., 1967. "On a linear instability of a plane parallel couette flow of viscoelastic fluid". *Journal of Applied Mathematics and Mechanics*, Vol. 31, pp. 289–299.

Han, C.D., 1976. *Rheology in Polymer Processing*. Academic Press, New York.

Keiller, R.A., 1992. "Numerical instability of time-dependent flows". *Journal of Non-Newtonian Fluid Mechanics*, Vol. 43, pp. 229–246.

Kloker, M., 1998. "A robust high-resolution split-type compact fd scheme for spatial direct numerical simulation of boundary-layer transition". *Applied Scientific Research*, Vol. **59**, pp. 353–377.

Kloker, M., Konzelmann, U. and Fasel, H.F., 1993. "Outflow boundary conditions for spatial navier-stokes simulations of transition boundary layers". *AIAA Journal*, Vol. **31**, pp. 620–628.

Lele, S., 1992. "Compact finite difference schemes with spectral-like resolution". *J. Comput. Phys.*, Vol. **103**, pp. 16–42.

Lieu, B.K., Jovanovic, M.R. and KUMAR, S., 2013. "Worst-case amplification of disturbances in inertialess couette flow of viscoelastic fluids". *Journal of Fluid Mechanics*, Vol. 723, pp. 232–263.

Palmer, A., 2007. *Linear Stability Analyses of Poiseuille Flows of Viscoelastic Liquids*. Ph.D. thesis, The University of Wales, Aberystwyth, United Kingdom.

Porteous, K.C. and Denn, M.M., 1972a. "Linear stability of plane poiseuille flow of viscoelastic liquids". *Transactions of The Society of Rheology*, Vol. 16, pp. 295–308.

Porteous, K.C. and Denn, M.M., 1972b. "Nonlinear stability of plane poiseuille flow of viscoelastic liquids". *Transactions of The Society of Rheology*, Vol. 16, pp. 309–319.

Rogenski, J.K., Petri, L.A. and Souza, L.F., 2015. "Effects of parallel strategies in the transitional flow investigation". *Journal of the Brazilian Society of Mechanical Sciences and Engineering*, Vol. 37, pp. 861–Ű872.

Souza, L.F., 2003. *Instabilidade Centrífuga e transição para turbulência em Escoamentos Laminares Sobre Superfícies Côncavas*. Ph.D. thesis, Instituto Tecnológico de Aeronáutica.

Souza, L.F., Mendonça, M.T. and Medeiros, M.A.F., 2005. "The advantages of using high-order finite differences schemes in laminar-turbulent transition studies". *International Journal for Numerical Methods in Fluids*, Vol. **48**, pp. 565–592.

Stüben, K. and Trottenberg, U., 1981. *Nonlinear multigrid methods, the full approximation scheme*, Köln-Porz, chapter 5, pp. 58–71.

Sureshkumar, R., 2001. "Local linear stability characteristics of viscoelastic periodic channel flow". *Journal of Non-Newtonian Fluid Mechanics*, Vol. 97, pp. 125–148.

Sureshkumar, R., Smith, M.D., Armstrong, R.C. and Brown, R.A., 1999. "Linear stability and dynamics of viscoelastic flows using time-dependent numerical simulations". *Journal of Non-Newtonian Fluid Mechanics*, Vol. 82, pp. 57–104.

Yih, C.S., 1967. "Instability due to viscosity stratification". *Journal of Fluid Mechanics*, Vol. 27, pp. 337–352.

Zhang, M., Lashgari, I., Zaki, T.A. and Brandt, L., 2013. "Linear stability analysis of channel flow of viscoelastic oldroyd-b and fene-p fluids". *Journal of Fluid Mechanics*, Vol. 737, pp. 249–279.

7. RESPONSIBILITY NOTICE

The authors are the only responsible for the printed material included in this paper.